# Inversion twinning in a second polymorph of the hydrochloride salt of the recreational drug ethylone

Cameron, T Stanley ; Grossert, J Stuart ; Maheux, Chad R ; Alarcon, Idralyn Q ; Copeland, Catherine R ; Linden, Anthony

DOI: https://doi.org/10.1107/S2053229615004295

STRUCTURAL CHEMISTRY

ISSN: 2053-2296
journals.iucr.org/c

# Inversion twinning in a second polymorph of the hydrochloride salt of the recreational drug ethylone

**T. Stanley Cameron, J. Stuart Grossert, Chad R. Maheux, Idralyn Q. Alarcon, Catherine R. Copeland and Anthony Linden**

*Acta Cryst.* (2015). C**71**, 266–270

Acta Cryst C STRUCTURAL CHEMISTRY

ISSN 2053-2296

# Inversion twinning in a second polymorph of the hydrochloride salt of the recreational drug ethylone

T. Stanley Cameron,[a]* J. Stuart Grossert,[a] Chad R. Maheux,[b] Idralyn Q. Alarcon,[b] Catherine R. Copeland[b] and Anthony Linden[c]*

[a]Department of Chemistry, Dalhousie University, PO Box 15000, Halifax, Nova Scotia, Canada B3H 4R2, [b]Science and Engineering Directorate, Canada Border Services Agency, 79 Bentley Avenue, Ottawa, Ontario, Canada K2E 6T7, and [c]Department of Chemistry, University of Zurich, Winterthurerstrasse 190, CH-8057 Zurich, Switzerland. *Correspondence e-mail: stanley.cameron@dal.ca, anthony.linden@chem.uzh.ch

Received 27 February 2015
Accepted 2 March 2015

Edited by A. L. Spek, Utrecht University, The Netherlands

**Keywords:** polymorphism; computational chemistry; twinning; ethylone; pharmaceutical compound; amphetamine analogue; crystal structure; hydrochloride salt; hydrogen bonding; DFT calculations; lattice energy calculations; absolute structure refinement.

**CCDC reference**: 1051738

**Supporting information**: this article has supporting information at journals.iucr.org/c

A second polymorph of the hydrochloride salt of the recreational drug ethylone, $C_{12}H_{16}NO_3^+\cdot Cl^-$, is reported [systematic name: (±)-2-ethylammonio-1-(3,4-methylenedioxyphenyl)propane-1-one chloride]. This polymorph, denoted form (*A*), appears in crystallizations performed above 308 K. The originally reported form (*B*) [Wood *et al.* (2015). *Acta Cryst.* C**71**, 32–38] crystallizes preferentially at room temperature. The conformations of the cations in the two forms differ by a 180° rotation about the C—C bond linking the side chain to the aromatic ring. Hydrogen bonding links the cations and anions in both forms into similar extended chains in which any one chain contains only a single enantiomer of the chiral cation, but the packing of the ions is different. In form (*A*), the aromatic rings of adjacent chains interleave, but pack equally well if neighbouring chains contain the same or opposite enantiomorph of the cation. The consequence of this is then near perfect inversion twinning in the structure. In form (*B*), neighbouring chains are always inverted, leading to a centrosymmetric space group. The question as to why the polymorphs crystallize at slightly different temperatures has been examined by density functional theory (DFT) and lattice energy calculations and a consideration of packing compactness. The free energy ($\Delta G$) of the crystal lattice for polymorph (*A*) lies some 52 kJ mol$^{-1}$ above that of polymorph (*B*).

## 1. Introduction

Ethylone [also called 3,4-methylenedioxy-*N*-ethylcathinone or (±)-1-(1,3-benzodioxol-5-yl)-2-(ethylamino)propan-1-one], (I), is controlled as an amphetamine analogue under the *Controlled Drugs and Substances Act* in Canada. Ethylone was patented in 1996 as an antidepressant (Jacob & Shulgin, 1996) and some analytical data were published shortly thereafter in an effort to rapidly identify this compound should it appear in the underground drug market (Dal Cason, 1997). However, two different polymorphic forms of the hydrochloride salt of ethylone, herein labelled (*A*) and (*B*), were discovered when seized exhibits of ethylone hydrochloride intercepted at the Canadian border were found to have different spectroscopic data (FT–IR, FT–Raman and powder X-ray diffraction) compared with those from a synthesized reference standard (Maheux *et al.*, 2015). We have found that different methods of preparation of ethylone hydrochloride at room temperature produced large block-shaped crystals of form (*B*), small crystals of form (*A*) that were not suitable for crystallography, or a mixture of both. Polymorph (*A*) appears as very small fine needle crystals. A typical large specimen among these small crystals measured 0.5 × 0.5 × 15.0 µm. If (*A*) is recrystallized at a temperature above 308 K, then polymorph (*A*) persists.

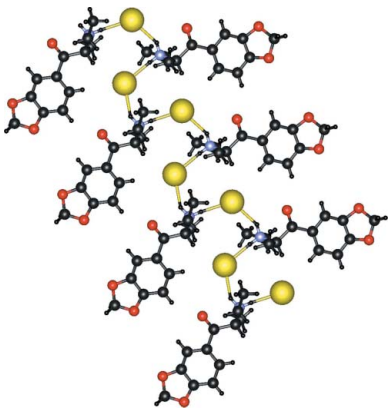

After many recrystallization attempts, it was found that if solid (*A*) was left in contact with a saturated solution of the compound in a 50:50 *v*/*v* water–methanol mixture [essentially damp crystals, since (*A*) is very soluble] and this mixture was left in a temperature cycler for a period of more than four weeks, then ultimately a few needle-shaped crystals up to 0.3 mm long and of a quality just suitable for an X-ray crystal structure determination were obtained. We report here the crystal structure of (*A*) at 160 K, together with a comparison with the structure of (*B*) at 100 K, which has been reported recently (Wood *et al.*, 2015), although we have also determined the structure of (*B*) at 160 K, at room temperature and at 313 K and found no phase change across this temperature range. We also consider reasons why there are two polymorphs and suggest why they might form at different temperatures.

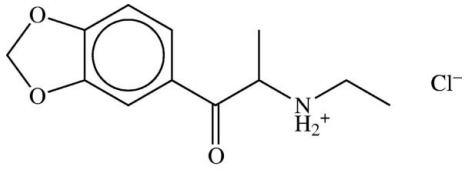


(I)·HCl

## 2. Experimental

### 2.1. Synthesis and crystallization

Samples of synthesized and seized ethylone hydrochloride were supplied by the Canada Border Services Agency. A small sample of polymorph (*A*) was dissolved in a methanol–water mixture (50:50 *v*/*v*) and allowed to evaporate slowly in a temperature cycler that raised and lowered the temperature of the solution over the range 308–311 K, with each complete cycle (308–311–308 K) lasting about 40 min. When very little liquid was left, the vial was sealed tightly and the temperature cycling continued for four weeks. The final result contained many very fine needles, but among the lumps a few larger needle-shaped crystals were found, the largest of these were approximately 0.04 × 0.05 × 0.30 mm and were (just) suitable for X-ray crystal structure determination.

### 2.2. Refinement

Crystal data, data collection and structure refinement details are summarized in Table 1. All H atoms were placed in geometrically idealized positions and constrained to ride on their parent atoms, with N—H = 0.91 Å and C—H = 0.95 (aromatic), 0.98 (methyl), 0.99 (methylene) and 1.00 Å (methine), and with $U_{iso}$(H) = 1.5$U_{eq}$(C) for the methyl groups and 1.2$U_{eq}$(C,N) otherwise. Initial refinement of the completed structure model yielded an absolute structure parameter of 0.497 (12), based on the quotients method (Parsons *et al.*, 2013), which indicated the presence of an inversion twin. For the final refinements, the TWIN/BASF instructions were included in the *SHELXL2014* instruction file (Sheldrick, 2015), so as to include the contribution of both twin components to the structure-factor calculations during the least-squares optimization, and the major twin fraction refined to 0.50 (5). This procedure is important when an inversion twin has been detected, because, in the absence of these instructions, the absolute structure parameter calculated by *SHELXL2014* is only done post-refinement, without including the contribution from the inverse model in the least-squares calculations. When the absolute structure parameter deviates significantly from zero and its standard uncertainty is sufficiently small for the value to be meaningful, failure to include TWIN/BASF in the refinement can lead to bias in the final model. In this case, refinement without TWIN/BASF led to $R[F^2 > 2\sigma(F^2)]$ = 0.069, compared with the lower value of 0.067 associated with the reported refinement results for which these instructions were included.

**Table 1**
Experimental details.

| | |
|---|---|
| Crystal data | |
| Chemical formula | $C_{12}H_{16}NO_3^+\cdot Cl^-$ |
| $M_r$ | 257.71 |
| Crystal system, space group | Orthorhombic, $P2_12_12_1$ |
| Temperature (K) | 160 |
| *a*, *b*, *c* (Å) | 6.90225 (16), 7.13000 (16), 25.4692 (5) |
| *V* (Å$^3$) | 1253.42 (5) |
| *Z* | 4 |
| Radiation type | Cu *Kα* |
| $\mu$ (mm$^{-1}$) | 2.69 |
| Crystal size (mm) | 0.30 × 0.06 × 0.03 |
| Data collection | |
| Diffractometer | Oxford Diffraction SuperNova (dual radiation) diffractometer |
| Absorption correction | Gaussian (*CrysAlis PRO*; Agilent, 2014) |
| $T_{min}$, $T_{max}$ | 0.707, 0.923 |
| No. of measured, independent and observed [$I > 2\sigma(I)$] reflections | 7202, 2421, 2286 |
| $R_{int}$ | 0.032 |
| (sin $\theta/\lambda)_{max}$ (Å$^{-1}$) | 0.626 |
| Refinement | |
| $R[F^2 > 2\sigma(F^2)]$, $wR(F^2)$, *S* | 0.067, 0.180, 1.11 |
| No. of reflections | 2421 |
| No. of parameters | 157 |
| H-atom treatment | H-atom parameters constrained |
| $\Delta\rho_{max}$, $\Delta\rho_{min}$ (e Å$^{-3}$) | 0.74, −0.34 |
| Absolute structure | Refined as an inversion twin using 929 Friedel pairs |
| Absolute structure parameter | 0.50 (5) |

Computer programs: *CrysAlis PRO* (Agilent, 2014), *SHELXS2014* (Sheldrick, 2008), *ORTEPII* (Johnson, 1976), *Mercury* (Macrae *et al.*, 2008), *CrystalStructure* (Rigaku, 2007), *SHELXL2014* (Sheldrick, 2015) and *PLATON* (Spek, 2015).

## 3. Results and discussion

Ethylone, (I), is constructed from an aromatic planar 1,3-benzodioxole [1,2-(methylenedioxy)benzene] unit with a C(O)C(CH$_3$)NHCH$_2$CH$_3$ side chain at the 4-position of the benzene ring. In the hydrochloride salt of ethylone, the N atom of the free base is protonated (see Scheme). Polymorph (*A*) of the hydrochloride salt crystallizes in the space group $P2_12_12_1$ with one cation and a chloride anion in the asymmetric unit (Fig. 1). The cation contains a chiral C atom (C8),

**Table 2**
Hydrogen-bond geometry (Å, °).

| $D$—H···$A$ | $D$—H | H···$A$ | $D$···$A$ | $D$—H···$A$ |
|---|---|---|---|---|
| N1—H1···Cl1 | 0.91 | 2.24 | 3.149 (4) | 174 |
| N1—H2···Cl1$^{i}$ | 0.91 | 2.30 | 3.134 (5) | 153 |

Symmetry code: (i) $-x, y-\frac{1}{2}, -z+\frac{3}{2}$.

yet the compound is a racemate and in the chosen crystal crystallizes as a perfect inversion twin. The two $NH_2^+$ H atoms hydrogen bond to two symmetry-related $Cl^-$ ions, with H···Cl distances of 2.24 and 2.30 Å (Table 2). This links the ammonium groups of the cations to the anions in an alternating sequence into a simple zigzag chain that propagates parallel to the [010] direction and can be described by a graph-set motif of $C_2^1(4)$ (Bernstein *et al.*, 1995). The direction of the hydrogen-bonded chains corresponds to the needle axis of the crystal (*b* axis). The alkyl groups of the cations are directed towards the core of the chain, while the planar aromatic groups of adjacent cations within the chain are disposed alternately on opposite sides of the chain core (Fig. 1*b*) and, in the crystal, these planar groups lie almost exactly on and parallel to the (100) plane. Fig. 2 shows a view of the crystal packing projected down [010] parallel to the chain axis, so, for example, the bottom left shows the chain spiralling along a $2_1$ screw axis going into the page. Adjacent chains along the [100] direction are simply repeats by a unit-cell translation. If one such sequence of parallel chains is considered, then the aromatic groups slot neatly between those from the neighbouring equivalent sequences on either side in the [001] direction, although they are offset in the [010] direction to preclude the existence of $\pi$–$\pi$ stacking interactions. This is shown by the central vertical stack of aromatic groups in Fig. 2. This interleaving provides an explanation for both the formation of the inversion twin and the difficulty in growing a crystal of any size. In the crystal, each hydrogen-bonded chain is a unique enantiopure unit. Yet the next chain, formed in the crystal by the interleaving of the aromatic planar groups (left-to-right in Fig. 2), has no guiding requirement other than that all cations in that chain be the same enantiomorph; the packing is such that a chain need not contain the same enantiomorph as that in an adjacent chain. However, the chains above and below (top and bottom left in Fig. 2) will probably need to be composed of the same enantiomorph, thus the crystal will form enantiopure layers lying parallel to (001), but with each layer able to be composed of either one of the two enantiomorphs. This random packing of the layers of the two enantiomorphs will produce an inversion twin. Moreover, the very precise requirement within any one chain and layer of having a single enantiomorph within that chain and layer, while a cation of either enantiomorph can slip into any slot, makes construction of a layer a process potentially littered with errors, which lead to defects that have to be corrected before the crystal can grow to any size. If the errors were not corrected, the structure would necessarily be disordered, which is not observed with the crystal used for the measurements.

The structure of polymorph (*A*) described here was determined at 160 K. The structure has also been determined at room temperature where, apart from the expected differences caused by the rise in temperature, it is exactly the same as the low-temperature structure and there is no indication of a

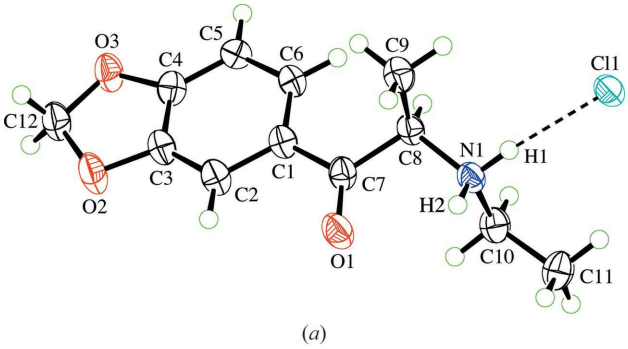


(*a*)

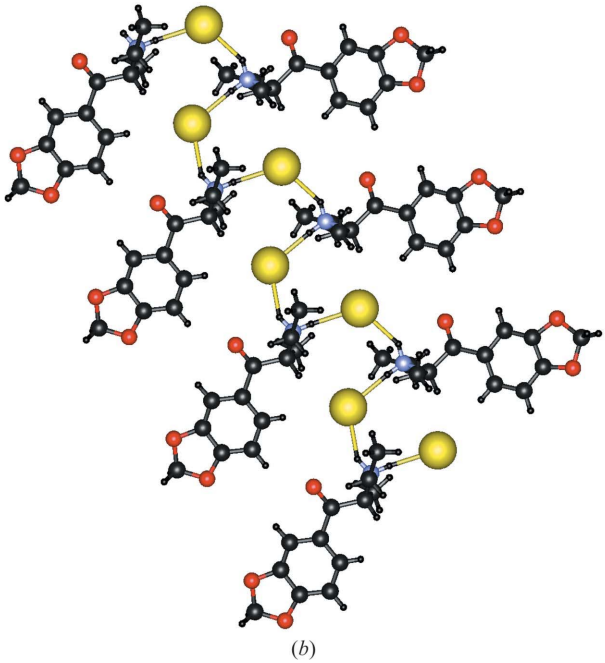

(*b*)

**Figure 1**
(*a*) The asymmetric unit of polymorph (*A*), showing the atom-labelling scheme and one of the hydrogen bonds linking the ions (dashed line). Displacement ellipsoids are drawn at the 50% probability level. (*b*) A hydrogen-bonded chain (yellow bonds) within the structure of polymorph (*A*).

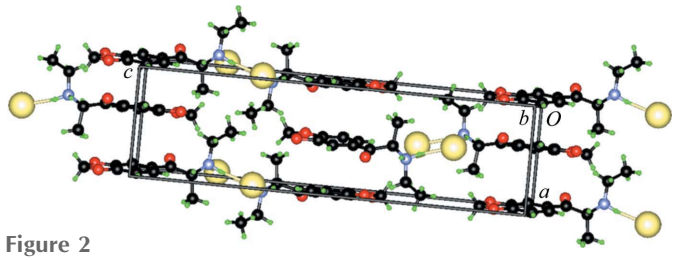


**Figure 2**
Packing in the unit cell of polymorph (*A*), viewed down the hydrogen-bonded chains (down [010]). Aromatic groups lie approximately parallel to the (100) plane; those from chains along the $2_1$ screw axes at $z = \frac{1}{4}, \frac{3}{4}$ interleave at $z = \frac{1}{2}$, although they are offset in the [010] direction.

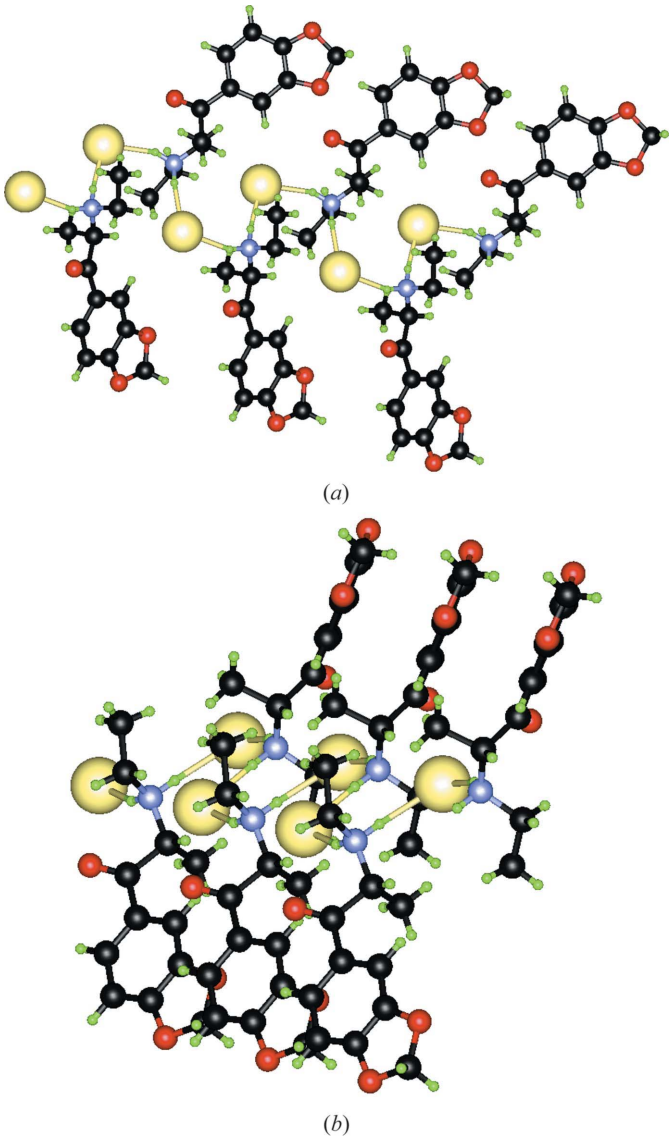


**Figure 3**
(*a*) A hydrogen-bonded chain (yellow bonds) within the structure of polymorph (*B*) (Wood *et al.*, 2015). (*b*) Close overlap of the aromatic rings within the hydrogen-bonded chain of polymorph (*B*).

phase change to polymorph (*B*). Similarly, the structure of polymorph (*B*) shows no indication of a phase change to polymorph (*A*) across the temperature range from 100 (Wood *et al.*, 2015) to 313 K, as mentioned above. Polymorph (*B*) crystallizes in the centrosymmetric space group $P2_1/c$ with thus both enantiomers present as a perfect racemate. The hydrogen-bonding scheme in (*B*), not described in detail by Wood *et al.* (2015), also produces a simple single chain sequence with the $C_2^1(4)$ motif (Fig. 3*a*), where the aromatic groups again alternate on opposite sides of the chain. Here, however, the cations are much more tightly concentrated so that the aromatic groups on each side of the chain are now tightly packed together (Figs. 3*a* and 3*b*) and there is no possibility of interleaving with an adjacent chain. Since the chain is of a zigzag nature and propagates along a $2_1$ screw axis, each chain, as expected, contains only one of the two

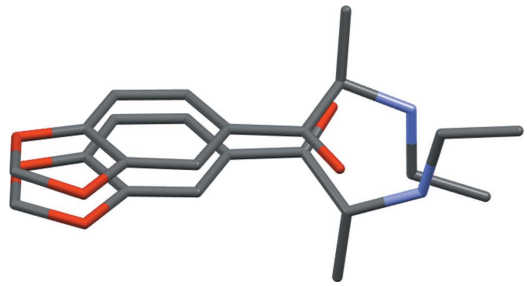

**Figure 4**
An overlay of the cations in polymorphs (*A*) and (*B*), showing the different conformation of the side chain. For clarity, the image of polymorph (*A*) is displaced slightly upwards.

enantiomorphs, while the chain related by the inversion centre contains the other enantiomorph.

Once the cations in each polymorph are examined, the reason for the two polymorphs is immediately obvious. The carbonyl group in polymorph (*A*) is oriented in the opposite direction with respect to its orientation in polymorph (*B*) relative to the fused-ring system. Essentially, the entire side chain is rotated by approximately 180° about the C1—C7 bond linking the side chain to the ring system (Fig. 4). Thus, each polymorph contains a completely different conformer. Given the considerable molecular reorganization required to change from one conformation to the other, it is not surprising that no phase change is observed in the solid state when moving from the preferred crystallization temperature of one polymorph to that of the other.

An examination of Figs. 1(*b*) and 3(*b*) shows a considerable difference between the arrangement of adjacent aromatic groups within the hydrogen-bonded chain of each of the two polymorphs. This is perhaps the result of $\pi$-stacking of the aromatic groups of adjacent cations for (*B*), which is not available for (*A*). In (*A*), the aromatic groups of the cations pack side-by-side along *b*, with very poor overlap with the groups in the cations above and below, while in the crystal of (*B*), pairs of aromatic groups from adjacent chains manage a reasonable overlap of the benzene rings at a centroid–centroid distance of 3.6174 (12) Å and a slippage of 1.15 Å [based on the data of Wood *et al.* (2015)].

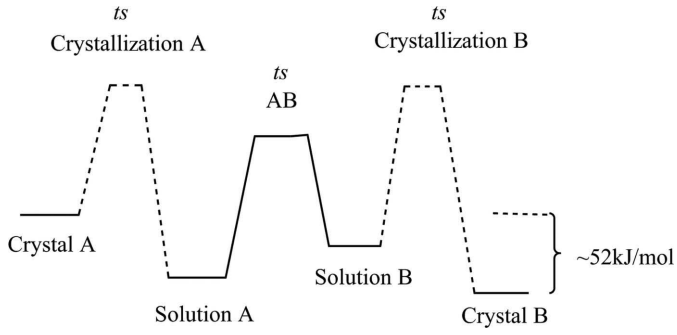


**Figure 5**
Energy changes from a crystal of polymorph (*A*) to a crystal of polymorph (*B*) through a solution in methanol/water (*ts* indicates the transition states).

Table 3
Relative free energies for polymorphs (*A*) and (*B*), as well as the rotational transition state TS(*AB*) in the gas phase [298 K, 1 atm (1 atm = 101 325 Pa)] and applying the self-consistent reaction field polarizable continuum model (SCRF-PCM) for methanol and water (298 K, 1 atm)[a].

| Computation | $\Delta G$ (kJ mol$^{-1}$) |
|---|---|
| (*A*), gas phase | 0 |
| (*AB*), gas phase | 34 |
| (*B*), gas phase | 35 |
| (*A*), MeOH | 0 |
| (*AB*), MeOH | 31 |
| (*B*), MeOH | 14 |
| (*A*), HOH | 0 |
| (*AB*), HOH | 30 |
| (*B*), HOH | 12 |

Note: (*a*) computations done at 288 and 318 K yielded essentially the same relative energies.

The remaining question is why polymorph (*A*) is formed at temperatures above 308 K, when (*B*) is preferred at, or below, room temperature (293 K). To examine this question we need to consider (*a*) the relative solvation energies for the two conformers of the ammonium cations, plus the solvation energy of the chloride ion, (*b*) the activation energy barrier for conversion of one conformer of the solvated ammonium cations into the other conformer, (*c*) the activation energy for the change from solution state to solid state, (*d*) the concentration of the two conformers when crystallization occurs, (*e*) the difference in the lattice energies of the two polymorphs, and (*f*) effects of spontaneous nucleation (Fig. 5).

Given the complexity of the methanol–water system used for crystallization, we did not investigate variable (*a*), other than to recognize that the solvation energies of the two conformers will be different. It has been noted that solvation of alkylammonium ions is different from that of the ammonium ion and is influenced by electrostatic nonlocal interactions involving the alkyl groups (Vallet & Masella, 2015).

Variable (*b*) was estimated using density functional theory (DFT) computations (*GAUSSIAN09*; Frisch *et al.*, 2010) using the wB97XD/6-311+g(d) level functional (Chai & Head-Gordon, 2008) and basis set. Solvation was modelled using the self-consistent reaction field polarizable continuum model (SCRF-PCM; Tomasi *et al.*, 2005) with the solvent set to the dielectric constants for either methanol or water. All structures were fully optimized and a frequency analysis was done also, which gave energy minima having no imaginary frequencies and transition states with one. The comparable gas-phase computations were made for comparison. Results giving the free energies ($\Delta G$) are given in Table 3. Thus, the transition state energy relative to the two conformers appears to be slightly higher in water and their solvation energies also reflect the differences in solvent polarity.

Variables (*c*) and (*d*) were deemed to be not quantifiable, but variable (*e*) could be computed. This was done using the CP2K computation suite for condensed matter (Hutter *et al.*, 2014) at the PBE+D3(TZV2PX) level. The computations were done within periodic boundary conditions with four cations and four anions per unit cell (132 atoms), with pseudopotentials for all atoms and 376 valence electrons per unit cell. These computations showed that the free energy ($\Delta G$) of the crystal lattice for polymorph (*A*) was some 52 kJ mol$^{-1}$ greater than that of polymorph (*B*). Finally, variable (*f*) was also considered not to be quantifiable.

These energy values in conjunction with the recrystallization observations suggest a plausible explanation for the formation of the two polymorphs. At the higher recrystallization temperature in the methanol–water system, the single cation with the anion of the (*A*) conformer, which is more stable in solution than that of the (*B*) conformer, dominates. At this higher temperature, with the moderate activation energy barrier for the (*B*) conformer to change to (*A*), the (*A*) polymorph is formed. As the temperature falls, the cations and anions start to aggregate and at this point the more compact aggregate (compare Figs. 1*b* and 3*b*) favours the more stable crystal structure, which is (*B*), and the (*B*) polymorph is formed.

## Acknowledgements

We are deeply grateful to Professor J. Hutter, University of Zurich, for performing the CP2K computations and B. Millier, Dalhousie University, for construction of the temperature cycler.

## References

Agilent (2014). *CrysAlis PRO*. Agilent Technologies, Yarnton, Oxfordshire, England.
Bernstein, J., Davis, R. E., Shimoni, L. & Chang, N.-L. (1995). *Angew. Chem. Int. Ed. Engl.* **34**, 1555–1573.
Chai, J.-D. & Head-Gordon, M. (2008). *Phys. Chem. Chem. Phys.* **10**, 6615–6620.
Dal Cason, T. A. (1997). *Forensic Sci. Int.* **87**, 9–53.
Frisch, M. J. *et al.* (2010). *GAUSSIAN09*. Gaussian Inc., Wallingford, CT, USA. http://www.gaussian.com.
Hutter, J., Iannuzzi, M., Schiffmann, F. & VandeVondele, J. (2014). *WIREs Comput. Mol. Sci.* **4**, 15–25.
Jacob, P. III & Shulgin, A. T. (1996). US Patent WO1996039133 A1.
Johnson, C. K. (1976). *ORTEPII*. Report ORNL-5138. Oak Ridge National Laboratory, Tennessee, USA.
Macrae, C. F., Bruno, I. J., Chisholm, J. A., Edgington, P. R., McCabe, P., Pidcock, E., Rodriguez-Monge, L., Taylor, R., van de Streek, J. & Wood, P. A. (2008). *J. Appl. Cryst.* **41**, 466–470.
Maheux, C. R., Alarcon, I. Q., Copeland, C. R., Cameron, T. S., Linden, A. & Grossert, S. J. (2015). In preparation.
Parsons, S., Flack, H. D. & Wagner, T. (2013). *Acta Cryst.* B**69**, 249–259.
Rigaku (2007). *CrystalStructure*. Rigaku Corporation, The Woodlands, Texas, USA.
Sheldrick, G. M. (2008). *Acta Cryst.* A**64**, 112–122.
Sheldrick, G. M. (2015). *Acta Cryst.* C**71**, 3–8.
Spek, A. L. (2015). *Acta Cryst.* C**71**, 9–18.
Tomasi, J., Mennucci, B. & Cammi, R. (2005). *Chem. Rev.* **105**, 2999–3093.
Vallet, V. & Masella, M. (2015). *Chem. Phys. Lett.* **618**, 168–173.
Wood, M. R., Lalancette, R. A. & Bernal, I. (2015). *Acta Cryst.* C**71**, 32–38.

# supporting information

*Acta Cryst.* (2015). C**71**, 266-270 [doi:10.1107/S2053229615004295]

# Inversion twinning in a second polymorph of the hydrochloride salt of the recreational drug ethylone

**T. Stanley Cameron, J. Stuart Grossert, Chad R. Maheux, Idralyn Q. Alarcon, Catherine R. Copeland and Anthony Linden**

## Computing details

Data collection: *CrysAlis PRO* (Agilent, 2014); cell refinement: *CrysAlis PRO* (Agilent, 2014); data reduction: *CrysAlis PRO* (Agilent, 2014); program(s) used to solve structure: *SHELXS2014* (Sheldrick, 2008); program(s) used to refine structure: *SHELXL2014* (Sheldrick, 2015); molecular graphics: *ORTEPII* (Johnson, 1976), *Mercury* (Macrae *et al.*, 2008) and *CrystalStructure* (Rigaku, 2007); software used to prepare material for publication: *SHELXL2014* (Sheldrick, 2015) and *PLATON* (Spek, 2015).

### [1-(1,3-Benzodioxol-5-yl)-1-oxopropan-2-yl]ethanaminium chloride

*Crystal data*

$C_{12}H_{16}NO_3^+ \cdot Cl^-$
$M_r$ = 257.71
Orthorhombic, $P2_12_12_1$
$a$ = 6.90225 (16) Å
$b$ = 7.13000 (16) Å
$c$ = 25.4692 (5) Å
$V$ = 1253.42 (5) Å$^3$
$Z$ = 4
$F(000)$ = 544
$D_x$ = 1.366 Mg m$^{-3}$
Cu $K\alpha$ radiation, $\lambda$ = 1.54184 Å
Cell parameters from 3179 reflections
$\theta$ = 6.4–73.0°
$\mu$ = 2.69 mm$^{-1}$
$T$ = 160 K
Needle, pale yellow
0.30 × 0.06 × 0.03 mm

*Data collection*

Oxford Diffraction SuperNova (dual radiation) diffractometer
Radiation source: SuperNova (Cu) X-ray Source
Mirror monochromator
Detector resolution: 10.3801 pixels mm$^{-1}$
$\omega$ scans
Absorption correction: gaussian (*CrysAlis PRO*; Agilent, 2014)
$T_{min}$ = 0.707, $T_{max}$ = 0.923
7202 measured reflections
2421 independent reflections
2286 reflections with $I > 2\sigma(I)$
$R_{int}$ = 0.032
$\theta_{max}$ = 74.8°, $\theta_{min}$ = 3.5°
$h$ = −8→8
$k$ = −8→8
$l$ = −31→31

*Refinement*

Refinement on $F^2$
Least-squares matrix: full
$R[F^2 > 2\sigma(F^2)]$ = 0.067
$wR(F^2)$ = 0.180
$S$ = 1.11
2421 reflections
157 parameters
0 restraints
Hydrogen site location: inferred from neighbouring sites
H-atom parameters constrained

$w = 1/[\sigma^2(F_o^2) + (0.1079P)^2 + 1.0836P]$
where $P = (F_o^2 + 2F_c^2)/3$
$(\Delta/\sigma)_{max} = 0.001$
$\Delta\rho_{max} = 0.74$ e Å$^{-3}$
$\Delta\rho_{min} = -0.34$ e Å$^{-3}$
Absolute structure: Refined as an inversion twin using 929 Friedel pairs
Absolute structure parameter: 0.50 (5)

*Special details*

**Experimental**. Solvent used: 50:50 v.v. MeOH-H2O Cooling Device: Oxford Instruments Cryojet XL Crystal mount: on a glass fibre Frames collected: 2184 Seconds exposure per frame: 5.0–75.0 Degrees rotation per frame: 0.5 Crystal-detector distance (mm): 55.0 Client: Stan Cameron Sample code: ethlone hydrochloride (L1407)

**Geometry**. All e.s.d.'s (except the e.s.d. in the dihedral angle between two l.s. planes) are estimated using the full covariance matrix. The cell e.s.d.'s are taken into account individually in the estimation of e.s.d.'s in distances, angles and torsion angles; correlations between e.s.d.'s in cell parameters are only used when they are defined by crystal symmetry. An approximate (isotropic) treatment of cell e.s.d.'s is used for estimating e.s.d.'s involving l.s. planes.

**Refinement**. Refined as a 2-component inversion twin using 929 Friedel pairs

*Fractional atomic coordinates and isotropic or equivalent isotropic displacement parameters (Å$^2$)*

| | *x* | *y* | *z* | $U_{iso}$*/$U_{eq}$ |
|---|---|---|---|---|
| Cl1 | −0.0103 (2) | 0.35002 (17) | 0.80071 (4) | 0.0414 (4) |
| O1 | 0.1371 (7) | 0.1702 (6) | 0.58409 (15) | 0.0469 (10) |
| O2 | 0.0680 (8) | 0.4897 (6) | 0.40324 (15) | 0.0494 (11) |
| O3 | 0.0217 (6) | 0.8065 (5) | 0.41849 (13) | 0.0424 (9) |
| N1 | 0.1330 (7) | 0.2704 (6) | 0.68548 (16) | 0.0335 (9) |
| H1 | 0.0832 | 0.2945 | 0.7179 | 0.040* |
| H2 | 0.1048 | 0.1491 | 0.6774 | 0.040* |
| C1 | 0.0643 (8) | 0.4676 (8) | 0.54772 (19) | 0.0337 (11) |
| C2 | 0.0773 (9) | 0.3968 (8) | 0.4959 (2) | 0.0393 (12) |
| H21 | 0.0992 | 0.2676 | 0.4889 | 0.047* |
| C3 | 0.0565 (8) | 0.5253 (8) | 0.45632 (19) | 0.0360 (12) |
| C4 | 0.0302 (7) | 0.7116 (7) | 0.46539 (19) | 0.0333 (11) |
| C5 | 0.0214 (7) | 0.7849 (7) | 0.51485 (18) | 0.0319 (10) |
| H5 | 0.0059 | 0.9156 | 0.5206 | 0.038* |
| C6 | 0.0361 (7) | 0.6590 (7) | 0.55644 (18) | 0.0323 (10) |
| H6 | 0.0268 | 0.7042 | 0.5914 | 0.039* |
| C7 | 0.0879 (8) | 0.3315 (8) | 0.59123 (19) | 0.0343 (10) |
| C8 | 0.0363 (8) | 0.3947 (7) | 0.64665 (17) | 0.0311 (11) |
| H8 | 0.0811 | 0.5267 | 0.6520 | 0.037* |
| C9 | −0.1808 (9) | 0.3853 (9) | 0.6540 (2) | 0.0436 (14) |
| H91 | −0.2247 | 0.2557 | 0.6493 | 0.065* |
| H92 | −0.2442 | 0.4660 | 0.6280 | 0.065* |
| H93 | −0.2141 | 0.4281 | 0.6894 | 0.065* |
| C10 | 0.3466 (8) | 0.2923 (8) | 0.6877 (2) | 0.0389 (12) |
| H101 | 0.3792 | 0.4244 | 0.6957 | 0.047* |
| H102 | 0.4031 | 0.2608 | 0.6530 | 0.047* |
| C11 | 0.4327 (9) | 0.1655 (9) | 0.7293 (2) | 0.0441 (13) |
| H111 | 0.3945 | 0.0355 | 0.7224 | 0.066* |
| H112 | 0.3850 | 0.2036 | 0.7640 | 0.066* |
| H113 | 0.5742 | 0.1755 | 0.7285 | 0.066* |
| C12 | 0.0225 (9) | 0.6636 (8) | 0.37870 (19) | 0.0437 (12) |

| | | | | |
|---|---|---|---|---|
| H121 | −0.1062 | 0.6562 | 0.3617 | 0.052* |
| H122 | 0.1203 | 0.6934 | 0.3515 | 0.052* |

*Atomic displacement parameters (Å²)*

| | $U^{11}$ | $U^{22}$ | $U^{33}$ | $U^{12}$ | $U^{13}$ | $U^{23}$ |
|---|---|---|---|---|---|---|
| Cl1 | 0.0673 (8) | 0.0288 (6) | 0.0282 (5) | 0.0097 (6) | 0.0067 (6) | 0.0024 (4) |
| O1 | 0.075 (3) | 0.033 (2) | 0.0327 (18) | 0.004 (2) | 0.0023 (18) | −0.0044 (16) |
| O2 | 0.080 (3) | 0.043 (2) | 0.0249 (17) | −0.005 (2) | 0.0033 (18) | −0.0025 (16) |
| O3 | 0.059 (2) | 0.042 (2) | 0.0267 (16) | −0.006 (2) | 0.0019 (16) | 0.0035 (14) |
| N1 | 0.046 (2) | 0.027 (2) | 0.0273 (18) | 0.0010 (18) | 0.0011 (17) | −0.0015 (16) |
| C1 | 0.037 (2) | 0.036 (3) | 0.028 (2) | −0.005 (2) | 0.0015 (19) | −0.001 (2) |
| C2 | 0.051 (3) | 0.037 (3) | 0.030 (2) | −0.006 (2) | 0.003 (2) | −0.003 (2) |
| C3 | 0.040 (3) | 0.042 (3) | 0.026 (2) | −0.006 (2) | 0.0033 (19) | −0.002 (2) |
| C4 | 0.033 (2) | 0.037 (3) | 0.030 (2) | −0.008 (2) | 0.0016 (18) | 0.0057 (19) |
| C5 | 0.033 (2) | 0.029 (2) | 0.034 (2) | −0.002 (2) | 0.003 (2) | 0.0005 (18) |
| C6 | 0.035 (2) | 0.034 (2) | 0.028 (2) | −0.004 (2) | 0.0006 (17) | −0.0041 (19) |
| C7 | 0.043 (2) | 0.032 (3) | 0.028 (2) | −0.005 (2) | −0.0032 (19) | −0.001 (2) |
| C8 | 0.046 (3) | 0.021 (2) | 0.026 (2) | −0.003 (2) | −0.0004 (19) | −0.0007 (16) |
| C9 | 0.048 (3) | 0.050 (4) | 0.033 (3) | 0.000 (3) | 0.004 (2) | −0.001 (2) |
| C10 | 0.043 (3) | 0.040 (3) | 0.033 (2) | −0.005 (2) | 0.001 (2) | 0.002 (2) |
| C11 | 0.050 (3) | 0.044 (3) | 0.038 (3) | −0.005 (3) | −0.004 (2) | 0.009 (2) |
| C12 | 0.059 (3) | 0.044 (3) | 0.027 (2) | −0.005 (3) | 0.000 (2) | 0.000 (2) |

*Geometric parameters (Å, º)*

| | | | |
|---|---|---|---|
| O1—C7 | 1.213 (7) | C5—H5 | 0.9500 |
| O2—C3 | 1.378 (6) | C6—H6 | 0.9500 |
| O2—C12 | 1.424 (7) | C7—C8 | 1.524 (7) |
| O3—C4 | 1.374 (6) | C8—C9 | 1.511 (8) |
| O3—C12 | 1.437 (6) | C8—H8 | 1.0000 |
| N1—C10 | 1.484 (7) | C9—H91 | 0.9800 |
| N1—C8 | 1.486 (6) | C9—H92 | 0.9800 |
| N1—H1 | 0.9100 | C9—H93 | 0.9800 |
| N1—H2 | 0.9100 | C10—C11 | 1.515 (8) |
| C1—C6 | 1.396 (7) | C10—H101 | 0.9900 |
| C1—C2 | 1.417 (7) | C10—H102 | 0.9900 |
| C1—C7 | 1.482 (7) | C11—H111 | 0.9800 |
| C2—C3 | 1.369 (8) | C11—H112 | 0.9800 |
| C2—H21 | 0.9500 | C11—H113 | 0.9800 |
| C3—C4 | 1.360 (8) | C12—H121 | 0.9900 |
| C4—C5 | 1.365 (7) | C12—H122 | 0.9900 |
| C5—C6 | 1.392 (7) | | |
| | | | |
| C3—O2—C12 | 104.9 (4) | N1—C8—C7 | 109.6 (4) |
| C4—O3—C12 | 105.3 (4) | C9—C8—C7 | 109.5 (4) |
| C10—N1—C8 | 114.1 (4) | N1—C8—H8 | 109.4 |
| C10—N1—H1 | 108.7 | C9—C8—H8 | 109.4 |

| | | | |
|---|---|---|---|
| C8—N1—H1 | 108.7 | C7—C8—H8 | 109.4 |
| C10—N1—H2 | 108.7 | C8—C9—H91 | 109.5 |
| C8—N1—H2 | 108.7 | C8—C9—H92 | 109.5 |
| H1—N1—H2 | 107.6 | H91—C9—H92 | 109.5 |
| C6—C1—C2 | 120.4 (5) | C8—C9—H93 | 109.5 |
| C6—C1—C7 | 122.5 (4) | H91—C9—H93 | 109.5 |
| C2—C1—C7 | 117.2 (5) | H92—C9—H93 | 109.5 |
| C3—C2—C1 | 116.1 (5) | N1—C10—C11 | 110.7 (4) |
| C3—C2—H21 | 121.9 | N1—C10—H101 | 109.5 |
| C1—C2—H21 | 121.9 | C11—C10—H101 | 109.5 |
| C4—C3—C2 | 122.9 (5) | N1—C10—H102 | 109.5 |
| C4—C3—O2 | 110.7 (5) | C11—C10—H102 | 109.5 |
| C2—C3—O2 | 126.3 (5) | H101—C10—H102 | 108.1 |
| C3—C4—C5 | 122.4 (5) | C10—C11—H111 | 109.5 |
| C3—C4—O3 | 109.8 (4) | C10—C11—H112 | 109.5 |
| C5—C4—O3 | 127.7 (5) | H111—C11—H112 | 109.5 |
| C4—C5—C6 | 116.9 (5) | C10—C11—H113 | 109.5 |
| C4—C5—H5 | 121.6 | H111—C11—H113 | 109.5 |
| C6—C5—H5 | 121.6 | H112—C11—H113 | 109.5 |
| C5—C6—C1 | 121.3 (4) | O2—C12—O3 | 108.0 (4) |
| C5—C6—H6 | 119.4 | O2—C12—H121 | 110.1 |
| C1—C6—H6 | 119.4 | O3—C12—H121 | 110.1 |
| O1—C7—C1 | 122.7 (5) | O2—C12—H122 | 110.1 |
| O1—C7—C8 | 119.0 (5) | O3—C12—H122 | 110.1 |
| C1—C7—C8 | 118.2 (5) | H121—C12—H122 | 108.4 |
| N1—C8—C9 | 109.7 (4) | | |

| | | | |
|---|---|---|---|
| C6—C1—C2—C3 | −1.3 (8) | C2—C1—C6—C5 | −0.4 (8) |
| C7—C1—C2—C3 | −179.5 (5) | C7—C1—C6—C5 | 177.6 (5) |
| C1—C2—C3—C4 | 1.8 (8) | C6—C1—C7—O1 | −170.2 (5) |
| C1—C2—C3—O2 | 178.5 (5) | C2—C1—C7—O1 | 7.9 (8) |
| C12—O2—C3—C4 | −7.2 (6) | C6—C1—C7—C8 | 13.5 (7) |
| C12—O2—C3—C2 | 175.8 (6) | C2—C1—C7—C8 | −168.3 (5) |
| C2—C3—C4—C5 | −0.4 (9) | C10—N1—C8—C9 | −170.5 (4) |
| O2—C3—C4—C5 | −177.5 (5) | C10—N1—C8—C7 | 69.3 (5) |
| C2—C3—C4—O3 | 177.6 (5) | O1—C7—C8—N1 | 23.9 (7) |
| O2—C3—C4—O3 | 0.5 (7) | C1—C7—C8—N1 | −159.8 (4) |
| C12—O3—C4—C3 | 6.4 (6) | O1—C7—C8—C9 | −96.4 (6) |
| C12—O3—C4—C5 | −175.8 (5) | C1—C7—C8—C9 | 79.9 (6) |
| C3—C4—C5—C6 | −1.4 (8) | C8—N1—C10—C11 | 178.2 (4) |
| O3—C4—C5—C6 | −179.1 (5) | C3—O2—C12—O3 | 10.9 (6) |
| C4—C5—C6—C1 | 1.8 (7) | C4—O3—C12—O2 | −10.7 (6) |

*Hydrogen-bond geometry (Å, º)*

| *D*—H···*A* | *D*—H | H···*A* | *D*···*A* | *D*—H···*A* |
|---|---|---|---|---|
| N1—H1···Cl1 | 0.91 | 2.24 | 3.149 (4) | 174 |

| | | | | |
|---|---|---|---|---|
| N1—H2···Cl1$^{i}$ | 0.91 | 2.30 | 3.134 (5) | 153 |

Symmetry code: (i) $-x$, $y-1/2$, $-z+3/2$.